

# $H_2$ Control for Active Suspension to Improve Ride Comfort based on ISO 2631

M2015SC015 Kohei SUZUKI

Supervisor : Isao TAKAMI

## Abstract

This paper presents a method of  $H_2$  control for an active suspension to improve the ride comfort based on ISO 2631. The half-car model is used to analyze the vertical motion and pitch motion. The time delay between front and rear wheels is approximated by using the Pade approximation and high pass filter. Based on the frequency weighting curves and the multiplying factors in ISO, the evaluated function is designed. The effectiveness of the proposed method is verified by simulations and experiments.

## 1 INTRODUCTION

A suspension is a shock absorber between car body and wheels. There are a passive suspension and an active suspension. The passive suspension absorbs the vibration from the road surface by using springs and dampers. The active suspension shows the higher performance than passive one by using an actuator in addition to the springs and the dampers.

In this study, the  $H_2$  controller is proposed to improve the ride comfort based on ISO 2631. The half-car model, which can analyze the vertical motion and the pitch motion, is used. To improve the ride comfort based on ISO 2631, this study approaches by two methods. The first one is Pade approximation for the time delay. The time delay is important for the analysis of ride comfort because the pitch motion depends on the disturbance timings between front and rear wheels. The time delay for the disturbance between front wheel and rear wheel is approximated by using the first-order Pade approximation. However, when the first-order Pade approximation is used, the high frequency bands of the vertical acceleration is underestimated for the original time delay. Then, the pitch angular acceleration is approximated based on the resonance point of the original time delay. On the other hand, when the second-order Pade approximation is used, the vertical acceleration is approximated based on the resonance point of the original time delay. However, the pitch angular acceleration is underestimated for the original time delay. Based on the frequency response of vertical acceleration with the second-order Pade approximations, the high pass filter is designed to shape the response of the first-order Pade approximation. The second method is loop-shaping based on ISO 2631. The most uncomfortable frequency bands are the ranges of 4-8[Hz] for the vertical acceleration and 0.6-0.8[Hz] for the pitch angular acceleration, respectively. By designing the frequency weights based on these frequency bands, the loop-shaping is applied to the vertical acceleration and the pitch angular acceleration. The weighted accelerations are evaluated by the ratio of 10 : 4 called multiplying factors in ISO 2631. The  $H_2$  controller, which can improve the response for the impulse disturbance, is designed. The effectiveness of proposed method is illustrated by simulations and experiments.

## 2 MODELING

The characteristics of the half-car model are discussed. The half-car model, which consists of two mass-spring-damper systems, is shown in Fig. 1. To analyze the vertical motion and the pitch motion, the front side and rear side of the car body is connected by the negligible bar of gravity. There is an actuator between the car body and wheel. When the actuator is stopped, the active suspension model works as the passive suspension model.

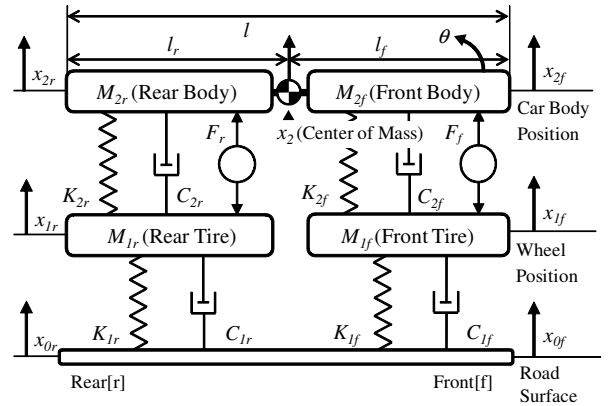


Figure 1: Half-Car Model

### 2.1 Physical Constants

The physical constants in the half-car model are shown based on an experimental unit. The car body position  $x_2$  and the wheel position  $x_1$  are considered as the displacements from the equilibrium points. The pitch angle of the car body is  $\theta$ . The front and rear control inputs are  $F_f$  and  $F_r$ . The physical constants are shown in Tab. 1. The parameters with suffix  $f$  and suffix  $r$  stand for the front side and rear side of the half-car model, respectively. The front and rear lengths of the car body are derived as  $l_f = M_{2r}l/(M_{2f} + M_{2r})$  and  $l_r = M_{2f}l/(M_{2f} + M_{2r})$ , respectively.

Table 1: Physical Constants

Unsprung mass	$M_{1f}$	$M_{1r}$	[kg]
Sprung mass	$M_{2f}$	$M_{2r}$	[kg]
Wheel stiffness	$K_{1f}$	$K_{1r}$	[N/m]
Suspension stiffness	$K_{2f}$	$K_{2r}$	[N/m]
Wheel damping	$C_{1f}$	$C_{1r}$	[Ns/m]
Suspension damping	$C_{2f}$	$C_{2r}$	[Ns/m]
Wheelbase (Length of car body)	$l$		[m]

### 2.2 Motion Equations

The motion equations of the half-car model are derived by using Newton's motion equation. The nonlinear terms,  $\sin \theta$  and  $\cos \theta$ , are approximated as  $\sin \theta \approx \theta$  and  $\cos \theta \approx 1$ . The motion equations of  $x_{1f}$ ,  $x_{1r}$ ,  $x_2$ ,

and  $\theta$  are derived as Eqs. (1) to (4), respectively.

$$\begin{aligned} M_{1f}\ddot{x}_{1f} = & -K_{1f}(x_{1f} - x_{0f}) - C_{1f}(\dot{x}_{1f} - \dot{x}_{0f}) \\ & + K_{2f}(x_{2f} - x_{1f}) + C_{2f}(\dot{x}_{2f} - \dot{x}_{1f}) \\ & - F_f \end{aligned} \quad (1)$$

$$\begin{aligned} M_{1r}\ddot{x}_{1r} = & -K_{1r}(x_{1r} - x_{0r}) - C_{1r}(\dot{x}_{1r} - \dot{x}_{0r}) \\ & + K_{2r}(x_{2r} - x_{1r}) + C_{2r}(\dot{x}_{2r} - \dot{x}_{1r}) \\ & - F_r \end{aligned} \quad (2)$$

$$\begin{aligned} M_2\ddot{x}_2 = & -K_{2f}(x_{2f} - x_{1f}) - C_{2f}(\dot{x}_{2f} - \dot{x}_{1f}) \\ & - K_{2r}(x_{2r} - x_{1r}) - C_{2r}(\dot{x}_{2r} - \dot{x}_{1r}) \\ & + F_f + F_r \end{aligned} \quad (3)$$

$$\begin{aligned} M_{2f}M_{2r}l\ddot{\theta} = & + M_{2f}K_{2r}(x_{2r} - x_{1r}) \\ & - M_{2r}C_{2f}(\dot{x}_{2f} - \dot{x}_{1f}) + M_{2r}F_f \\ & - M_{2r}K_{2f}(x_{2f} - x_{1f}) \\ & + M_{2f}C_{2r}(\dot{x}_{2r} - \dot{x}_{1r}) - M_{2f}F_r \end{aligned} \quad (4)$$

Here,  $M_2$  means the sum of the car body weights,  $M_{2f} + M_{2r}$ . The time delay  $\tau$ [s] between front disturbance and rear disturbance is calculated as  $\tau = l/(V \cdot 1000/3600)$  from the wheelbase  $l$ [m] and vehicle speed  $V$ [km/h].

### 3 CONTROLLER SYNTHESIS

The controller is designed to improve the ride comfort based on ISO 2631 [1]. The suspension dynamics  $P(s)$  is derived from the motion equations. The time delay  $e^{-s\tau}$  is approximated as the rational transfer function  $D_1(s)$  and the high pass filter  $F(s)$  by using Pade approximation. The frequency weight  $W(s)$  is designed based on the frequency weighting curves in ISO. The designed plants are integrated as the extended system  $G(s)$ . The evaluation outputs for the vertical acceleration and the pitch angler acceleration are evaluated based on the multiplying factors in ISO. The  $H_2$  controller is designed by solving LMIs.

#### 3.1 Suspension Dynamics $P(s)$

The state space representation  $P(s)$  including the suspension dynamics is derived from the motion equations. The state variable vector  $x(t)$ , the output vector  $y(t)$ , the disturbance vector  $w(t)$ , and the control input vector  $u(t)$  are defined as Eqs. (5) to (8).

$$x(t) = [ \begin{matrix} x_{1f} - x_{0f} & x_{1r} - x_{0r} & x_{2f} - x_{1f} & x_{2r} - x_{1r} \\ \dot{x}_{1f} & \dot{x}_{1r} & \dot{x}_{2f} & \dot{x}_{2r} \end{matrix} ]^T \quad (5)$$

$$y(t) = [ \begin{matrix} y_1(t) & y_2(t) \end{matrix} ]^T = [ \begin{matrix} \ddot{x}_2 & \ddot{\theta} \end{matrix} ]^T \quad (6)$$

$$w(t) = [ \begin{matrix} w_f(t) & w_r(t) \end{matrix} ]^T = [ \begin{matrix} \dot{x}_{0f} & \dot{x}_{0r} \end{matrix} ]^T \quad (7)$$

$$u(t) = [ \begin{matrix} F_f & F_r \end{matrix} ]^T \quad (8)$$

The state space representation  $P(s)$  is defined as Eq. (9).

$$P(s) : \begin{cases} \dot{x}(t) = Ax(t) + B_{1f}w_f(t) + B_{1r}w_r(t) + B_2u(t) \\ y(t) = Cx(t) + Du(t) \end{cases} \quad (9)$$

#### 3.2 Time Delay $e^{-s\tau}$

The time delay  $e^{-s\tau}$  from the front disturbance  $w_f(t)$  to the rear disturbance  $w_r(t)$  is approximated by using Pade approximation [2]. Because the pitch motion depends on the disturbance timings between front and rear wheels, the time delay affects the ride comfort. The first-order Pade approximation  $D_1(s)$  and the second-order

Pade approximation  $D_2(s)$  for time delay  $e^{-s\tau}$  are derived as Eqs. (10) and (11), respectively.

$$D_1(s) = \frac{w_r(s)}{w_f(s)} = \frac{2 - \tau s}{2 + \tau s} \quad (10)$$

$$D_2(s) = \frac{w_r(s)}{w_f(s)} = \frac{12 - 6\tau s + \tau^2 s^2}{12 + 6\tau s + \tau^2 s^2} \quad (11)$$

When the first-order Pade approximation  $D_1(s)$  is used for time delay  $e^{-s\tau}$ , the high frequency band of the vertical acceleration is underestimated, but the pitch angular acceleration is accurately approximated for all frequency band. On the other hand, when the second-order Pade approximation  $D_2(s)$  is used for time delay  $e^{-s\tau}$ , all frequency band of the vertical acceleration is accurately approximated, but the pitch angular acceleration isn't underestimated for the high frequency band. To shape the high frequency bands of the vertical acceleration for the first-order Pade approximation  $D_1(s)$ , the high pass filter  $F(s)$  is designed as block diagram Fig. 2. Here,  $P_w(s)$  means the transfer function  $P(s)$  from

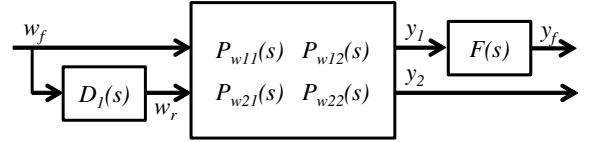


Figure 2: Time Delay  $D_1(s)$  and High Pass Filter  $F(s)$

disturbance  $w(t)$  as Eq. (12).

$$\begin{bmatrix} y_1(s) \\ y_2(s) \end{bmatrix} = \begin{bmatrix} P_{w11}(s) & P_{w12}(s) \\ P_{w21}(s) & P_{w22}(s) \end{bmatrix} \begin{bmatrix} w_f(s) \\ w_r(s) \end{bmatrix} \quad (12)$$

The high pass filter  $F(s)$  is derived based on the first-order Pade approximation  $D_1(s)$  and the second-order Pade approximation  $D_2(s)$  as Eq. (13).

$$\begin{aligned} F(s) = & (P_{w11}(s) + P_{w12}(s)D_2(s)) \\ & (P_{w11}(s) + P_{w12}(s)D_1(s))^{-1} \\ = & (1 + D_2(s))(1 + D_1(s))^{-1} \\ = & \frac{4(6 - \tau s)}{\tau^2 s^2 + 6\tau s + 12} + \tau s \end{aligned} \quad (13)$$

$$\approx \frac{T_1 s + 1}{T_2 s + 1} \quad (14)$$

Here, the plant  $P(s)$  has the characteristic  $P_{w11}(s) = P_{w12}(s)$  because the front and rear weights of car body are considered as the same weights,  $M_{2f} = M_{2r}$ . The high pass filter  $F(s)$  (Eq. (13)) is approximated as the first-order rational transfer function (14). The first-order Pade approximation  $D_1(s)$  and high pass filter  $F(s)$  are translated into the state space representations (15) and (16).

$$D_1(s) : \begin{cases} \dot{x}_d(t) = A_d x_d(t) + B_d w_f(t) \\ w_r(t) = C_d x_d(t) + D_d w_f(t) \end{cases} \quad (15)$$

$$F(s) : \begin{cases} \dot{x}_f(t) = A_f x_f(t) + B_f y_1(t) \\ y_f(t) = C_f x_f(t) + D_f y_1(t) \end{cases} \quad (16)$$

#### 3.3 Frequency Weight $W(s)$

The frequency weight  $W(s)$  is designed based on the frequency weighting curves in ISO 2631. According to

the frequency weighting curves in ISO, the most uncomfortable frequency bands for the vertical acceleration and the pitch angular acceleration are in the range of 4-8 [Hz] and 0.6-0.8 [Hz], respectively. The frequency weights  $W_1(s)$  and  $W_2(s)$  for these accelerations are designed based on ISO. The frequency responses of the frequency weights,  $W_1(s)$  and  $W_2(s)$ , are shown in Fig. 3. The frequency weights for vertical acceleration and pitch

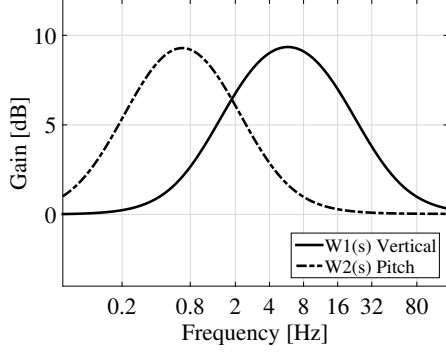


Figure 3: Frequency Weights  $W_1(s)$  and  $W_2(s)$

angular acceleration have the peak at 4-8[Hz] and 0.6-0.8[Hz], respectively. These frequency weights,  $W_1(s)$  and  $W_2(s)$ , are defined as the state space representation  $W(s)$  of MIMO.

$$W(s) : \begin{cases} \dot{x}_w(t) = A_w x_w(t) + B_w \tilde{y}(t) \\ y_w(t) = C_w x_w(t) + D_w \tilde{y}(t) \end{cases} \quad (17)$$

Here, the input vector  $\tilde{y}(t)$  including the vertical acceleration and pitch angular acceleration is defined as  $\tilde{y}(t) = [y_f(t) \quad y_2(t)]^T$ .

### 3.4 Extended System $G(s)$

The extended system  $G(s)$  is designed by introducing the new state variable vector  $x_g(t)$  and the evaluation output vector  $z(t)$  as Eqs. (18) and (19).

$$x_g(t) = [x(t) \quad x_d(t) \quad x_f(t) \quad x_w(t)]^T \quad (18)$$

$$z(t) = [u(t) \quad y_w(t)]^T \quad (19)$$

The new state space representation  $G(s)$  is derived as Eq. (20).

$$G(s) : \begin{cases} \dot{x}_g(t) = A_g x_g(t) + B_{1g} w_f(t) + B_{2g} u(t) \\ z(t) = C_g x_g(t) + D_g u(t) \end{cases} \quad (20)$$

The block diagram of the extended system  $G(s)$  is shown in Fig. 4.

### 3.5 Weight Matrix $W$

The weight matrix  $W$  is designed based on the multiplying factors in ISO 2631. The weighted accelerations for vertical acceleration and pitch angular acceleration are evaluated as the ratio of 10 : 4. The weight matrix  $W$  is designed as Eq. (21).

$$W = \text{diag}(W_1 \quad W_1 \quad W_2 \quad 0.4W_2) \quad (21)$$

By introducing the weight matrix  $W$ , the new evaluation output  $\tilde{z}(t)$  is defined as Eq. (22).

$$\begin{aligned} \tilde{z}(t) &= Wz(t) = WC_g x_g(t) + WD_g u(t) \\ &= \tilde{C}x_g(t) + \tilde{D}u(t) \end{aligned} \quad (22)$$

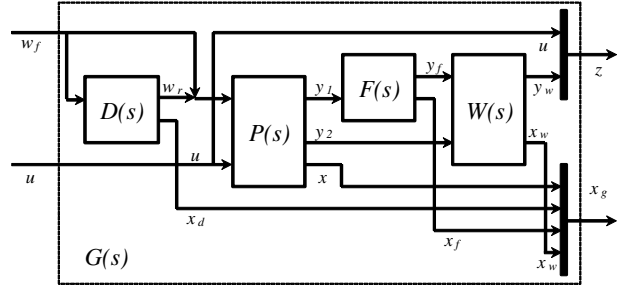


Figure 4: Extended System  $G(s)$

## 3.6 $H_2$ Controller

The state feedback controller is designed to improve the response for the disturbance. The situation that the car passes on the road surface of the step wise is considered. However, the disturbance  $w_f(t) = \dot{x}_0f(t)$  is defined as the vertical velocity of the road surface. When the road position is considered as the step wise disturbance, the vertical velocity of road surface is considered as impulse disturbance. The  $H_2$  controller, which can improve the response for the impulse disturbance, is designed.

## 4 SIMULATION & EXPERIMENT

The effectiveness of proposed controller is evaluated by simulations and experiments. The vehicle speed is considered as 50[km/h]. The weight matrix  $W$  is defined as  $W = \text{diag}(0.6 \quad 0.6 \quad 0.7 \quad 0.28)$ . The feedback gain  $K$  is obtained. The ride comfort is evaluated by comparing the proposed controller, the conventional controller, and the passive suspension. The conventional controller means the controller without the frequency weight  $W(s)$ .

### 4.1 Frequency Response (Simulation)

The ride comfort is evaluated by the frequency response. To evaluate the ride comfort exactly, the the frequency weighting curves in ISO are used for the vertical acceleration and pitch angular acceleration. The frequency weighting curves are defined as the transfer functions  $H_1(s)$  and  $H_2(s)$ . The transfer functions are integrated for the output equation  $y(t) = [y_1(t) \quad y_2(t)]^T$  in Fig. 5. The ride comfort is exactly evaluated by the

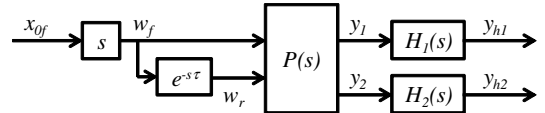


Figure 5: Analysis based on ISO

transfer functions  $\frac{y_{h1}(s)}{x_{0f}(s)}$  and  $\frac{y_{h2}(s)}{x_{0f}(s)}$ . Figs. 6 to 8 indicate the frequency response for the vertical acceleration, the pitch angular acceleration, and the total acceleration of these accelerations based on the multiplying factors, respectively. The solid line, the dashed line, and the dotted line indicate the proposed controller, the conventional controller, the passive suspension, respectively. As can be seen from the graph, the vertical acceleration and the pitch angular acceleration of the proposed controller are suppressed than the conventional controller and the passive suspension. The total acceleration for

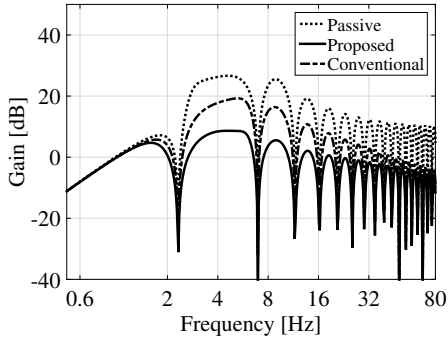


Figure 6: Vertical Acceleration

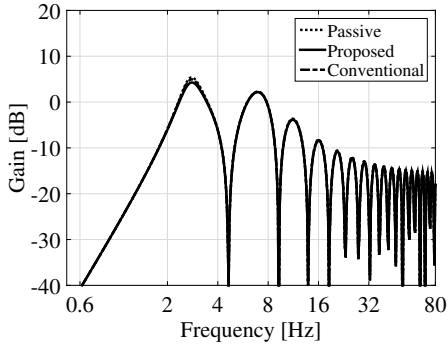


Figure 7: Pitch Angular Acceleration

proposed controller is suppress to about 32% at 6[Hz] for conventional controller.

#### 4.2 RMS Analysis (Simulation)

The ride comfort is evaluated by RMS acceleration based on ISO 2631. The overall RMS accelerations  $r_{w1}$  and  $r_{w2}$  for the vertical acceleration and the pitch angular acceleration are calculated as Eq. (23).

$$r_{w1} = \left[ \sum_j (r_{1j})^2 \right]^{\frac{1}{2}}, \quad r_{w2} = \left[ \sum_j (r_{2j})^2 \right]^{\frac{1}{2}} \quad (23)$$

Here,  $r_{1j}$  and  $r_{2j}$  indicate the RMS accelerations of weighted vertical acceleration and weighted pitch angular acceleration based on the  $j$ th one-third octave band in the range of 0.5-80[Hz]. The total RMS acceleration  $r_v$  is calculated as Eq. (24) based on the multiplying factors (ratio of 10 : 4).

$$r_v = \left[ r_{w1}^2 + (0.4r_{w2})^2 \right]^{\frac{1}{2}} \quad (24)$$

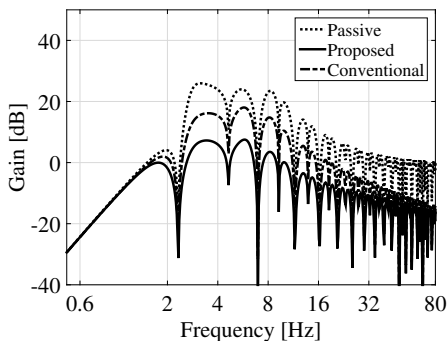


Figure 8: Total Acceleration

The RMS accelerations are shown as Tab. 2. As can be seen from the table, the total RMS acceleration for proposed controller is suppress to about 43% than conventional controller.

Table 2: RMS Accelerations

	Vertical	Pitch	Total
Passive Suspension	1.99	0.50	2.00
Conventional Controller	0.96	0.49	0.98
Proposed Controller	0.39	0.47	0.43

#### 4.3 Time Domain Analysis (Experiment)

The effectiveness of proposed controller is evaluated by the experiment of time domain analysis. The situation that the car passes on the square wave is considered. The period and amplitude of the square wave are 5[s] and 0.01[m], respectively. Fig. 9 indicates the experiment result of the vertical acceleration. The solid line

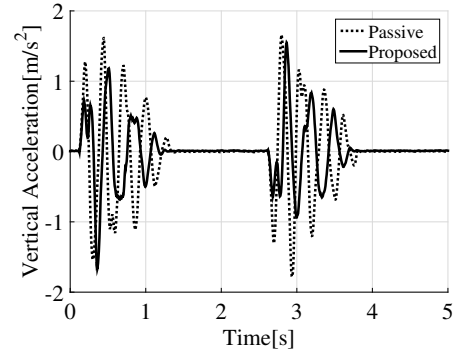


Figure 9: Experiment of Vertical Acceleration

and dotted line indicate the proposed controller and the passive suspension, respectively. As can be seen from the graph, the vertical acceleration for the proposed controller is improved than the passive suspension.

## 5 CONCLUSION

The method of  $H_2$  control for the active suspension is proposed to improve the ride comfort based on ISO 2631. The half-car model is used to analyze the vertical motion and the pitch motion. The time delay is approximated by using the first-order Pade approximation. To shape the vertical acceleration for the first-order Pade approximation, the high pass filter is designed. Based on the frequency weighting curves in ISO, the frequency weights are designed for the vertical acceleration and the pitch angular acceleration. The weighted accelerations are evaluated based on the multiplying factors in ISO. The effectiveness of the proposed controller is illustrated by simulations and experiments.

## References

- [1] ISO2631-1, Mechanical vibration and shock evaluation of human exposure to whole-body vibration Part 1 : General requirements, (1997)
- [2] T. Suzuki, M. Takahashi, Active Suspension Control Considering Lateral Vehicle Dynamics due to Road Input at Different Vehicle Speed (in Japanese), The Japan Society of Mechanical Engineers, Series C 78(786), pp.98-113, (2010)